Distributed Correlators for Interferometry in Space

Raj Thilak Rajan
National center for Radio Astronomy,
ASTRON, Dwingeloo, NL
rajan@astron.nl
and
Circuits and Systems, Faculty of ECMCS,
TU Delft, Delft, NL

Mark Bentum
National center for Radio Astronomy,
ASTRON, Dwingeloo, NL
bentum@astron.nl
and
Faculty of Electrical Engineering,
University of Twente, Enschede, The Netherlands

Andre Gunst
National center for Radio Astronomy,
ASTRON, Dwingeloo, NL
gunst@astron.nl

Albert-Jan Boonstra
National center for Radio Astronomy,
ASTRON, Dwingeloo, NL
boonstra@astron.nl

Abstract—**New and interesting science drivers have triggered a renewed interest in radio astronomy at ultra long wavelengths. However, at longer wavelengths (beyond 10 meters) ground-based radio astronomy is severely limited by Earths ionosphere, in addition to man-made interferences and solar flares. An unequivocal solution to the problem is to establish a space-based observatory for ultra low frequency (0.3MHz-30MHz) observations. In ground-based radio astronomy, interferometers comprising of widely spaced antennas are employed to enhance the sensitivity and angular resolution of the observations. The signals received from the antennas are pre-processed, phase corrected independently and then cross correlated with one another using a centralized correlator to estimate the coherence function. However, a space-based array, in addition to several other obstacles, presents new challenges for both communication and processing. In this paper, we discuss various conventional correlator architectures, such as *XF*, *FX* and *HFX*. In addition, the importance of a distributed correlator is emphasized for a space-based array, in particular Frequency distributed correlator. We compute transmission, reception and processing requirements for both centralized and distributed architecture. Finally, as a demonstration, we present 2 projects were these signal processing estimates are applied.**

TABLE OF CONTENTS

1. INTRODUCTION

Radio astronomy research in the last decades has contributed significantly to our understanding of the formation and evolution of the universe. At this moment the entire sky has been observed in detail in almost every band of the electromagnetic spectrum. However, there is still one major exception: the Ultra-Long Wavelength (ULW) radio band. This band is well suited for studying the early cosmos at high hydrogen redshifts, the so-called dark ages, extragalactic surveys, (extra) solar planetary bursts, transient radio sources , high energy particle physics and also in space research such as space weather [1]. While Earth based telescopes such as LOFAR (operating at 30-90 MHz, 120-240MHz [2]) and LWA (operating at 10-88 MHz [3]) cater to low frequencies, the spectrum below 10MHz has not been investigated due to two main reasons. The first reason is the ionosphere. Due to ionospheric scintillation (below 30MHz) and its opaqueness (below 15MHz, depending on the ionospheric conditions), Earth-bound radio astronomy observations in the ULW band are either severely limited in sensitivity and spatial resolution or entirely impossible. The second reason is the high impact of man-made interference and solar flares [4]. The only solution to open the last radio band for astronomy is building a radio telescope in space. Several concept studies and workshops have been started in the past [5], [6], [7], [8], however, until today no real ULW instrument is in operation yet. In the light of emerging technologies, new initiatives such as a radio telescope in space using very small satellites (e.g. nano-satellites). A nano-satellite typically has a mass of 10 Kg or less and is largely constructed from Commercial Off-The-Shelf (COTS) components. A consortium of universities and companies is currently investigating the feasibility of this concept. The future radio telescope has been named Orbiting Low Frequency Array (OLFAR) [9] [10]. OLFAR consist of an aperture synthesis interferometric array implemented with a swarm of nano-satellites ($\geq$ 10), in which each satellite carries one element of the array. The swarm will be deployed in a suitable orbit that provides the radio quietness required for the scientific observations. The satellite swarm concept consists in a system made up of simple autonomous units, which perform small tasks that contribute to the completion of a common system goal. In this paper the distributed data processing will be addressed in detail. In Figure 1 a schematic overview of OLFAR is presented. To limit the datastream to Earth, data processing is performed in space. After gathering the data, the data processing consists of correlation and/or beamforming, and time averaging. Several implementations are possible for each of the digital processing tasks, however in this paper we focus on distributed correlation. In Section 2 various conventional correlator architectures will be studied and in Section 3 the implementation choices of the correlator architecture will be discussed. As an illustration, the implementation of the digital signal processing part in the projects DARIS [11] and OLFAR [9] will be presented in Section 4. We summarize with some conclusions on the study.

Figure 1. Overview

Notation	Explanation	Comment
N_{stat}	Number of stations	stations/Nodes
N_{pol}	Number of polarizations	
N_{sig}	Number of signals	$N_{stat}N_{pol}$
N_{bits}	Number of bits	
N_{vis}	Number of visibilites	
N_X	Number of real multipliers	$N_{bits} \times N_{bits}$
N_{beams}	Number of beams	
N_{sb}	Number of subbands	
N_{bins}	Number of frequency bins	
N_{lags}	Number of frequency lags	$= N_{bins}$
τ_{int}	Correlation - integration time	
f_{sys}	Processing frequency	
Δf_o	Observation bandwidth	
Δf_i	Instantaneous bandwidth	$\Delta f_i \leq \Delta f_o$
Δf_{sb}	Sub-band bandwidth	$\Delta f_i / N_{sb}$

Table 1. Conventions

2. CORRELATION

In this paper, the key focus is to calculate three fundamental parameters *data in*, *data out* and *processing* for the DSP unit (Figure 1) for each satellite. The first order processing model estimates processing for correlation as the number of real $N_{bit} \times N_{bit}$ multipliers required for each mode, neglecting addition as a second order computation. Memory is another crucial factor, but is dependent on the implementation style on the hardware and hence will be ignored in this work. The signal processing system in all scenarios is assumed to run at rate f_{sys} and all the satellites are completely synchronized [12]. The complete list of conventions used is given in Table 1. In our estimation, we presume N_{stat} nodes (or satellites) with N_{pol} polarizations and subsequently the total number of signal paths N_{sig} is given as $N_{sig} = N_{stat}N_{pol}$. In the pre-processing block, each of these signals are conditioned, discretized and quantized at Nyquist rate $2 \times \Delta f_o$ where Δf_o is the total observational bandwidth. An instantaneous bandwidth of $\Delta f_i \leq \Delta f_o$ is then filtered for further processing. Thus a signal is a single polarization channel with base bandwidth of Δf_i which is coded with N_{bits} post quantization. In addition, in all the cases presented, it is assumed that the electrical and/or front end delays, geometrical delays have been compensated. Furthermore, the total number of multipliers required for generic signal processing tasks such
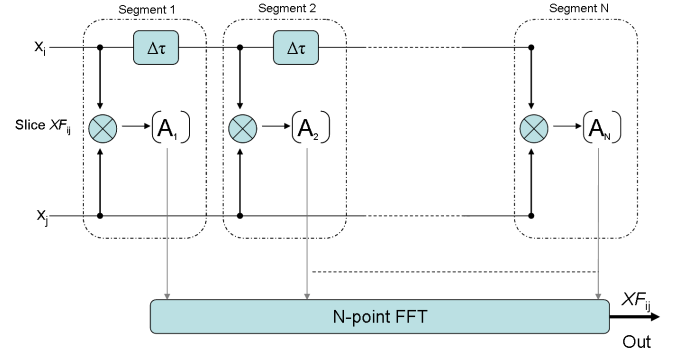
Figure 2. Single slice of Lag/ *XF* Correlator

as complex multiplication (17), Fast Fourier Transform (FFT) (19) and Poly-phase Filter Bank (PFB) (20) are calculated in Appendix and will be invoked often.

Correlation

Radio astronomers calculate the Fourier transform of the measured coherence function to make maps of the sky. Let $x_i(t)$ and $x_j(t)$ be two time varying signals received at spatial positions labeled i and j, then the coherence function $\zeta_{ij}(\tau)$ is the cross correlation product between and is given as

$$\zeta_{ij}(\tau_{int}) = \langle \, x_i(t)x_j^*(t - \tau_{ij}) \, \rangle_{\tau_{int}} \qquad (1)$$

where $\langle . \rangle$ is the expectation operator, the superscript $(*)$ indicates conjugation and τ_{ij} is the light travel time between observation of the same plane wave at the two antennae. The number of cross-correlation products increase as $O(N^2)$ for N antennas and the expectation operator is applied over a period of integration time τ_{int}. There are 3 ways to implement a correlator. The first option is using the traditional correlator model *XF* i.e. cross correlation first and Fourier transform later. The second alternative is the more recent *FX* correlator which measures the cross-power spectrum between two antenna signals. While *XF* architecture is beneficial because bandwidth can be traded for spectral resolution, *FX* architecture reduces processing requirements and offers scalability when the number of antennas is large. Finally, a combination of the *XF* and the *FX* architecture, yields an *HFX* correlator, where the data is first broken down into subbands and then each sub-band is analyzed by an XF correlator

XF *Correlator*

The conventional method to directly measure the cross-correlation function as indicated in (1) which forms the basis for the *XF* or 'Lag' correlator [13]. The signal $x_j(t)$ is delayed and correlated (X) with $x_i(t)$ to produce ζ_{ij} as a function of τ, which is later Fourier transformed (F) to produce the baseline cross power spectra. The cross correlation operation is a function of lags (τ), which could be varied in quantization of $n\Delta\tau$ where $-N_{lags}/2 \leq n < N_{lags}/2$, where for a given observation bandwidth Δf_o, $\Delta\tau$ is limited by $\Delta\tau_{min} = 1/(2 \times \Delta f_i)$. Consider a single slice XF_{ij} catering to baseline between antennae $\{i, j\}$ and containing $N = N_{lag}$ correlation segments as shown in Figure 2. The input signal x_i and the phase compensated x_j are the inputs to the correlator slice XF_{ij}. The signal x_j is delayed by $\Delta\tau$, multiplied and accumulated at every sample clock before propagating to the next segment. An *XF* correlation system will comprise of N_{sig} such slices with a total input bandwidth of $N_{sig}\Delta f_b N_{bits}$. For N_{sig} such slices, the total number of
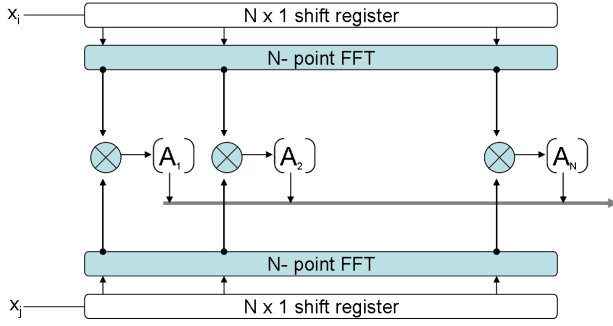
Figure 3. A 2-node *FX* Correlator

real multiplications per second is given from (1) and (17) is

$$N_X^{xf}/sec = N_X N_{lags} \Delta f_i = 2N_{sig}^2 N_{lags} \Delta f_i,$$

where $N_{sig} = N_{stat} N_{pol}$. If the system frequency is f_{sys} then the number of multipliers is given as

$$N_X^{xf} = 2N_{sig}^2 N_{lags} \left(\frac{\Delta f_i}{f_{sys}}\right). \quad (2)$$

An advantage of *XF* architecture is that the Fourier transform (FFT) operation can either be an online or an off-line process. This means that the correlator operates on the entire bandwidth for all nodes N_{stat} and the data generated can be tranmitted/stored without the immediate need to Fourier transform. Furthermore, since the FFT is an isomorphic process, the output rate is unaffected as shown in Table 2.

FX *Correlator*

An alternative to the *XF* correlator is to directly measure the cross-power spectrum. The term *FX* correlator was coined by Chikada [14] who built the first such correlator, implementing the reversal of the order of operations compared to the *XF* architecture. If $X_i(\nu)$ and $X_j(\nu)$ are the real time Fourier transforms of the delay compensated waveform $x_i(t)$ and $x_j(t)$ then using convolution theorem , the correlation function $\zeta_{ij}(\tau)$ in (1) can be written as a multiplication in the Fourier spectrum [15]

$$\zeta_{ij}(\tau) \;\Longleftrightarrow\; X_i(\nu) X_j^*(\nu)$$
$$\Longleftrightarrow\; X_{ij}(\nu). \quad (3)$$

Note that the cross-power spectrum to the right is a function of frequency and its Fourier transform to the left is a function of lags (τ). From implementation perspective, the essence is to transform each input signal x_i into frequency domain (*F*) and then multiply-accumulate (*X*) over each spectral bin for all the nodes, to produce the cross-power spectrum and later the visibility function off-line. Unlike the *XF* correlator, the *FX* correlator must do a node based Fourier transform on-line, as indicated in Figure 3. The number of points N, is given by the spectral resolution intended for the application

	No. of channels	bandwidth/channel	units
Input	N_{sig}	$2\Delta f_i N_{bits}$	(bits/sec)
Output	N_{lags}, N_{bins}	$2N_{sig}^2 N_{bits}/\tau_{int}$	(bits/sec)

Table 2. Data rates for Lag/ *XF* , *FX* and *HFX* correlator

i.e N_{bins}. A shift register loads N_{bins} samples which is Fourier transformed to produce N_{bins} points. The number of points N_{bins} can be interpreted as the spectral translation of N_{lags} from *XF* correlator in the time domain. The input and output data rates for such a system is given in Table 2. The total number of multipliers (N_X^{fx}) required is the sum of multipliers for node-based FFT (N_X^{fft}) and multipliers for Correlations (N_X^{corr}).

Consider N_{sig} signals inputted to the correlator block, then using a N_{bins} - point FFT processor for each signal and referring to eq(19) we have the total number of multipliers required as

$$N_X^{fft} = 2 N_{sig} \left(\frac{\Delta f_i}{f_{sys}}\right) \log_2 N_{bins}. \quad (4)$$

In contrast to the *XF* mode, where each sample is cross-multiplied at input rate, in *FX* mode each spectral bin is cross-multiplied and accumulated only once for N_{bins} samples, thereby reducing the number of computations by a factor N_{bins}. In other words, the cross-multipliers operate at a rate $(\Delta f_i/N_{bins})$ instead of Δf_i. From (17) we have , the number of multipliers required for correlation as

$$N_X^{corr} = 2N_{sig}^2 \left(\frac{\Delta f_i}{f_{sys}}\right). \quad (5)$$

The total number of multipliers for a N_{sig} input, N_{bins} *FX* correlator is then

$$\begin{aligned} N_X^{fx} &= N_X^{fft} + N_X^{corr} \\ &= 2N_{sig} \left(\frac{\Delta f_i}{f_{sys}}\right) [N_{sig} + \log_2 N_{bins}]. \quad (6) \end{aligned}$$

HXF *Correlator*

The *Hybrid XF* correlator splits the input bandwidth Δf_i into smaller sub-bands using a array of filters or filter banks, making it very similar to the *FX* implementation. A *XF* correlation operating at a lower data rate is then applied to each of the sub-bands. The input/output data rates in this case are the same as *XF* or the *FX* correlator module given in Table 2. The number of multipliers required to split the N_{sig} signals of bandwidth Δf_i into smaller N_{sb} sub-bands of width Δf_{sb} is given from (20)

$$N_X^{pfb} = 2N_{sig} \left(\frac{\Delta f_i}{f_{sys}}\right) [2N_{taps} + \log_2 N_{sb}], \quad (7)$$

where N_{taps} is the number of taps of the Poly-phase Filter Bank (PFB). In this mode a *XF* correlator operates on a single sub-band of band-width $\Delta f_i/N_{sb}$. However since there are N_{sb} such *XF* correlator modules, the total number of operations/sec for the entire process remains constant. The total number of multipliers is thus given from (2) and (7) we have

$$\begin{aligned} N_X^{hfx} &= N_X^{pfb} + N_X^{corr} \\ &= 2N_{sig} \left(\frac{\Delta f_i}{f_{sys}}\right) [N_{sig} + 2N_{taps} + \log_2 N_{sb}]. \end{aligned}$$

The hybrid modes effectively splits the large input baseband into non-overlapping sub-bands using PFBs and then applies *XF* [16]. This enables smaller sub-systems to operate on down sampled rates rather than on the entire band-width.
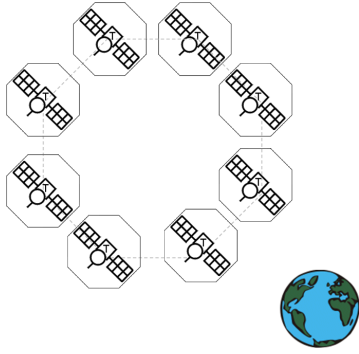
Figure 4. Raw Transmission

Summary

Processing factor XF/FX: The computational requirements of *XF* are much higher than *FX* mode for large number of nodes and higher spectral resolution. Comparing (2) and (6) we have the processing factor given as

$$N_X^{xf/fx} = \left(\frac{N_{sig} N_{bins}}{N_{sig} + \log_2 N_{bins}} \right). \tag{8}$$

As can be seen, the multiplicands in the *XF* mode are additive in the *FX* mode, besides the $\log_2$ reduction on the number of frequency bins. Thus, although for lower number of nodes the *XF* is comparable to *FX* mode, for large scalable architectures the *FX* mode is computationally cost effective. A similar reduction can be observed, by comparing the Hybrid mode against the *XF* mode,

$$N_X^{xf/hfx} = \left(\frac{N_{sig} N_{bins}}{N_{sig} + 2N_{taps} + \log_2 N_{bins}} \right), \tag{9}$$

which emphasizes the importance of breaking the bandwidth into smaller bands for processing. In addition, the *FX* and the *HFX* correlator also offers additional benefits such as fractional-sample delay compensation and truly station-based phase rotation. Hence, given the reduction in computations and additional benefits, we chose a *FX* correlator as our basis for correlator architecture design. The choice between the *FX* and *HFX* correlators depends on detailed parameters such as power consumption and flexibility of implementation.

3. CORRELATOR ARCHITECTURES

Among the three prevalent modes of correlation (*XF*, *FX*, *Hybrid*), the *FX* mode is assumed for all the below architectures.

Raw Transmission

The simplest scenario for a space-based interferometer is to transmit all the observed raw data to Earth. As illustrated in Figure 4, each satellite has transmission capability back to Earth, which is indicated with label 'T' and transmits $2N_{pol} \Delta f_i N_{bits}$ bits/sec. Observe that, with $N_{pol} = 3$, for a nominal instantaneous bandwidth of $\Delta f_i = 1$MHz for 1 bit correlation, each satellite must down-link 6 Mbits/sec to Earth. Given a far away deployment location, such as Lunar orbit ($\approx 384,000$ km), Earth-Moon L2 ($\approx 378,000$ km), Earth leading/trailing ($\approx 2 \times 10^6$ to 4×10^6 km), this down-link data rate levies heavy prerequisites on the resources of a small satellite. Hence, the satellite cluster must not only employ onboard pre-processing, but also onboard correlation

which is shown to minimize down-link data rate back to Earth.

Centralized Correlator

As the name suggests, the centralized correlator model, as shown in Figure 5, proposes to have a single correlation satellite for a cluster of $N_{stat} + 1$ satellites. The N_{stat} observation nodes are primarily responsible for transmitting the data to the centralized correlator node. Each satellite node transmits N_{pol} channels of capacity $2\Delta f_i N_{bits}$ bits/sec to the centralized mother ship, which receives at reception rate D_{in}^{cs}

$$D_{in}^{cs} = 2\Delta f_i N_{bits} N_{sig} \text{ (bits/sec)}. \tag{10}$$

The input data from all satellites is then correlated and the output is then down-linked/tranmitted down to Earth. Referring to (6) the total number of $N_{bit} \times N_{bit}$ multipliers needed per node are

$$N_X^{cs} = 2N_{sig} \left(\frac{\Delta f_i}{f_{sys}} \right) [N_{sig} + \log_2 N_{bins}]. \tag{11}$$

where $N_{sig} = N_{sig} N_{pol}$. After the correlation processes, the data is temporarily buffered and later transmitted down to Earth at scheduled intervals. Referring to Table 2, the data rate post-correlation is

$$D_{out}^{cs} = \left(\frac{2N_{sig}^2 N_{bins} N_{bits}}{\tau_{int}} \right) \text{ (bits/sec)}. \tag{12}$$

Distributed Correlator, Distributed Transmission

Centralized correlation depends heavily on the healthy operation of a single correlation node. Alternatively, the processing can be distributed to all nodes, removing the need for centralized correlation. This means that all antenna nodes take part in correlation. Additionally we also propose that after the processing each node down-links the data independently to Earth based node. Hence every node does both correlation and transmission denoted by 'XT' in the Figure 6. Three modes of distributing the signal processing for correlation are [17] (a) Antenna based distribution (b) Time based distribution and (c) Frequency based distribution. In Antenna based distribution, the entire data observed by each satellite is sent over to all other satellites for correlation. This immediately removes Single Point of Failure (SPoF), however increases communication and computation by incorporating high redundancy in the system. Alternatively, in Time based distribution, every satellite is assigned a particular time slot for correlation. This minimizes communication overload of the
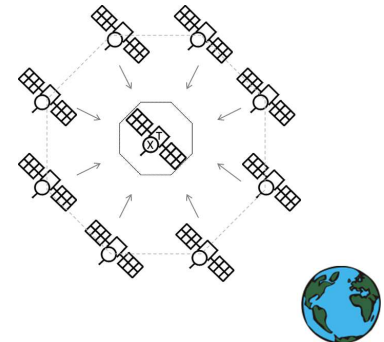
Figure 5. Centralized Correlator, Centralized Down-link
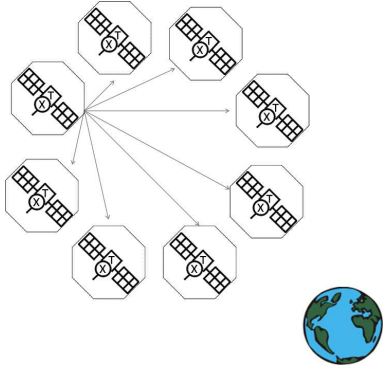
Figure 6. Distributed Correlator , Distributed Down-link

network by minimizing the data transmitted. However, this architecture requires high levels of coherent communication and processing between the satellites, which is an additional overload. The third alternative, which offers a truly distributed solution for correlation and optimal communication and processing is frequency distributed correlation.

Frequency distributed correlation—In this framework, each node is assigned to correlate a specific sub-band of the complete bandwidth Δf_i. Hence, after the preliminary signal conditioning and quantization, each node splits the instantaneous bandwidth Δf_i into N_{sb} subbands, each of bandwidth Δf_{sb}, such that $\Delta f_b = N_{sb}\Delta f_{sb}$. Each of these N_{sb} is then transmitted to the corresponding node assigned for that subband. For even distribution of data, we enforce the number of sub-bands equal to the number of nodes i.e

$$N_{sb} = N_{stat}. \tag{13}$$

Each satellite node receives N_{pol} channels each of bandwidth Δf_{sb} from all other $N_{stat} - 1$ nodes, with single sub-band of bandwidth f_{sb}. Thus, the total inter satellite reception rate for each node is given by

$$D_{in}^{fdc} = \Delta f_{sb}(N_{sb} - 1)N_{pol}N_{bits} \text{ (bits/sec/node)}. \tag{14}$$

Observe that the data transmission is reduced by a factor N_{sb} compared to the centralized correlation. In other words, every node transmits all the sub-bands of its input signal to all other nodes, except for the band it is assigned for correlation. In terms of processing, each satellite correlates only in a single sub-band Δf_{sb} and hence referring to (6) the number of $N_{bit} \times N_{bit}$ multipliers per node needed are

$$N_x{}^{fdc} = 2N_{sig}\left(\frac{\Delta f_{sb}}{f_{sys}}\right)[N_{sig} + log_2N_{bins}]. \tag{15}$$

Every node correlates a specific sub-band over a given integration time τ_{int} and then down-links the correlated data to Earth. From Table 2, the data rate of the final correlated output is given as

$$D_{out}^{fdc} = \left(\frac{N_{sig}^2N_{bins}N_{bits}}{\tau_{int}N_{stat}}\right) (bits/sec/node) \tag{16}$$

which, as expected, is a factor $N_{sb} = N_{stat}$ lower than the centralized correlator architecture and thereby dividing the communication resources evenly across all the satellite nodes. Evidently, if a single satellite fails, only a single sub-band

of the total observation is lost. Furthermore, given communication flexibility, other active satellites in the network can poll and reassign a larger sub-band, to retain sensitivity. Moreover, additional satellites can be added to the network to minimize communication overload and/or maximize instantaneous bandwidth.

Distributed Correlator, Centralized Transmission

Providing down-linking capability to all satellite nodes is an expensive task and in addition consumes valuable observation time . Alternatively, this can be avoided by adding a Transmitting node to the cloud of existing observation nodes N_{stat}. In this mode, aptly called Distributed Correlator- Centralized Transmission, the processing is distributed, but the downlink transmission is centralized. The total number of nodes are thus $N_{stat}^{tot} = N_{stat} + 1$. Since the processing is still
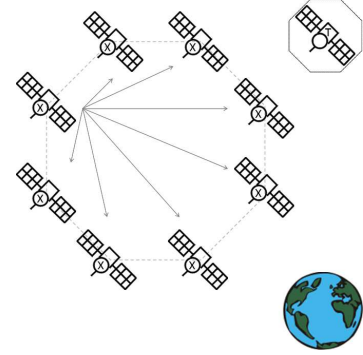
Figure 7. Distributed Correlator , Centralized Down-link

distributed, the equation for inter-satellite communication (14) and distributed processing given in (15) still hold. As shown in Figure 7, the centralized down-link node collects inter network processed data and down-links the processed data to Earth. The total data it receives is given from (10) and the down-link data rate is (12). Along similar lines, more down link satellites can be added to the cluster.

4. CASE STUDIES

To illustrate the distributed and centralized architectures discussed in the previous section, we investigate two feasibility studies, namely DARIS and OLFAR.

DARIS

DARIS is Distributed Aperture Array for Radio Astronomy in Space, a feasibility study to investigate a distributed aperture array in space for radio astronomy observations. The DARIS cluster comprises of 9 Nodes observing the cosmos in the ultra low frequency spectrum of $1 - 10$ MHz. Table 3 lists the first order requirements of the DARIS cluster. DARIS is an array of less than 10 nodes and is a feasibility study of a space-based array using Commercial Off-The-Shelf (COTS) components. Hence, although a distributed architecture is preferred, technology (in particular inter satellite communication) limits us to a centralized solution [11].

Node level Signal Processing for DARIS—Figure 8, shows a Node level Signal Processing (NSP) unit, which will be a part of all satellites in the DARIS cluster. Each of the observational satellite node will have $N_{pol} = 3$ separate data paths to the Node level Signal Processing (NSP) unit. Since the total observational bandwidth is too low, Direct Digital

	DARIS	OLFAR
Number of satellites (or antennas)	9 = 8 Nodes +1 Mother ship	≥ 10
Number of polarizations	3	3
Observation frequency range	0.3 - 10 MHz	0.3- 30 MHz
Instantaneous bandwidth	1MHz	≥ 1 MHz
Spectral resolution	1 kHz	1 kHz
Snapshot integration time	1 to 1000 s,	1 to 1000 s,
Maximum baseline between satellites	100 km	100 km
Deployment location	Earth orbit, Moon orbit, Moon far side, L2 point	Earth orbit, Moon orbit, Moon far side,
Processing (multipliers)	163	7.1 (per satellite)
Down link to Earth	1.4 MBits/sec	146KBits/sec/satellite

Table 3. DARIS and OLFAR system requirements
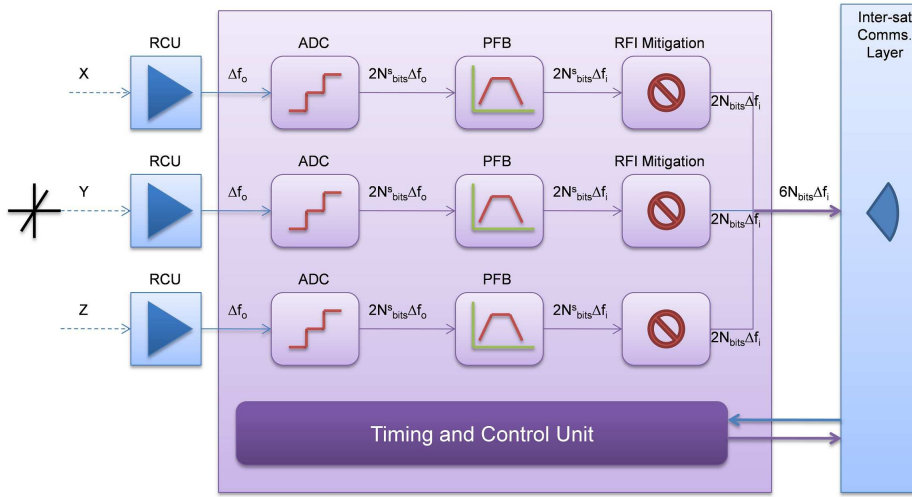
Figure 8. Node level Signal Processing (NSP) unit for DARIS

Conversion (DDC) is employed. This eliminates the need for mixing stages and IF to baseband conversion. Thus, the entire observational bandwidth of $\Delta f_o = 10$MHz input signal from each dipole is conditioned and directly sampled using a N_{bits}^s bits Analog to Digital Converter (ADC) at the Nyquist rate of $2\Delta f_o$. A coarsely Poly phase Filter Bank (PFB) [18] is used to selectively choose the desired instantaneous bandwidth of $\Delta f_i = \Delta f_o/N_{bins} = 1$ MHz [19]. The PFB is essentially a commutator, followed by an array of Finite Impulse Response (FIR) filters and an FFT block. This windowing prior using the FIR filters prior to the FFT block significantly improves the out-of-band rejection ratio of the obtained spectrum. Furthermore, RFI mitigation techniques can be employed to eliminate interference and reducing the total number of bits to $N_{bits} \leq N_{bits}^s$. The requirements of the dynamic range and hence N_{bits} will depend heavily on the deployment location of the satellites cluster [4]. However, we would assume a bare minimum of $N_{bits} = 1$ bits. The total amount of $N_{bit} \times N_{bit}$ multipliers for implementing the NSP for DARIS is given from (20) as $2\Delta f_o(2N_{taps} + \log_2 N_{bins})/f_{sys} = 71$, for $N_{taps} = 16$ and $f_{sys} = 10$MHz. The output from each signal processing data path will be $2\Delta f_i N_{bits} = 2$ Mbits/sec. For $N_{pol} = 3$ data paths, the total output from each satellite is $2N_{pol}\Delta f_i N_{bits} = 6$ Mbits/sec, which is sent to the intra satellite communication layer for transport. The centralized mother ship receives $2N_{stat}N_{pol}\Delta f_i N_{bits} = 48$ Mbits/sec,

where $N_{stat} = 8$ excluding the mother ship.

Centralized Processing and Down-link

As discussed earlier, the DARIS cluster will employ a centralized correlator- centralized down-link architecture. The centralized mother ship is also an observation satellite. Hence for correlating $N_{sig} = N_{pol}(N_{stat} + 1) = 27$ signal paths, the total number of processing units is given from (11) as $N_X^{daris} = 2N_{sig}\Delta f_i[N_{sig} + \log_2 N_{bins}]/f_{sys} = 163$ N_{bit} multipliers, given $f_{sys} = 10$ MHz. The Centralized mother ship then down-links data at the rate given by (12), as $D_{out}^{daris} = 2N_{sig}^2 N_{bins}N_{bits}/\tau_{int} = 1.46$ Mbits/sec.

OLFAR

The OLFAR (Orbiting Low Frequency Array for Radio astronomy) project aims to design and develop a detailed system concept for an un-tethered swarm of more than 10 scalable autonomous nano satellites in space (well above the ionosphere) to be used as a scientific instrument for ultra low frequency observations (Table 3). The large number of such satellites spread over large distances will collectively synthesize an aperture dish of diameter 100 kilometers. OLFAR is very similar in design to DARIS, however aims to observe a wider spectrum of $\Delta f_o \approx 30$ MHz and will consist of a

6

larger number of satellites. For the sake of illustration, we will consider a nominal $N_{stat} = 10$ satellites in this design.

Node level Signal Processing for OLFAR

Each observational satellite will be equipped with a NSP unit for preprocessing before correlation, which is shown in Figure 9. Along similar lines to the DARIS NSP, the input signal will be digitized, RFI mitigated (not shown in Figure 9) and filtered using a PFB to obtain the instantaneous bandwidth of $\Delta f_i = 1$MHz. In reality, OLFAR aims to achieve a larger instantaneous bandwidth $\geq$ 1MHz and thereby improving the sensitivity of the instrument. A second fine PFB is used to further split Δf_i into N_{sb} sub bands, each of bandwidth $\Delta f_{sb} = \Delta f_i/N_{sb}$. Furthermore, for even distribution of data, we enforce the number of sub-bands to be equal to the number of stations, $N_{sb} = N_{sat} = 10$ and hence $\Delta f_{sb} = 100$ Khz. The intra-satellite communication layer then transmits $N_{sb} - 1$ sub-bands to all other satellites. The number of multipliers required for the coarse PFB is similar to the DARIS PFB, which is 71 multipliers running at $f_{sys} = 10$ MHz and the for the Fine PFB, we have $2\Delta f_i[N_{sig} + \log_2 N_{bins}]/f_{sys} = 7.1$ multipliers, with $N_{taps} = 16$ in both cases. Each satellite then transmits $2N_{pol}(N_{sb} - 1)\Delta f_i = 5.4$ Mbits/sec to every other satellite in the network.

Distributed correlation and Down-link

The OLFAR network would employ Distributed correlation-Distributed down-link architecture, where by all the satellites will correlate data from a specific sub-band assigned to them. Using (15), each Node will employ $2N_{sig}\Delta f_{sb}[N_{sig} + \log_2 N_{bins}]/f_{sys} = 10$ multipliers, where $N_{sig} = N_{stat}N_{pol} = 30$. Observe that this requirement is an order smaller compared to the DARIS cluster of 9 nodes. Furthermore, from (16), each of the satellites will down-link the data at a factor of $N_{stat} = N_{sb}$ lower compared to the DARIS central mother ship, with $D_{out}^{olfar} = 2N_{sig}^2 N_{bins}N_{bits}/(N_{stat}\tau_{int}) = 146$ Kbits/sec/node.

5. CONCLUSION

A first order model of computational requirements for a correlator were presented, including an overview of conventional terrestrial correlator architectures such as *XF* , *FX* and *HFX* . For space-based intereferometry, centralized and distributed architectures were discussed, with emphasis on Frequency Distributed Correlation which is seen to be the optimal choice for a space-based array, distributing the downlink and processing evenly among all the satellite nodes, in addition to removing Single Point of Failure. As a computational illustration, the signal processing units of DARIS and OLFAR projects discussed, where centralized and distributed solutions are presented respectively.

APPENDIX

Complex Multiplications

The product of any 2 complex numbers; say $(x_1 + iy_1)$ and $(x_2 + iy_2)$ is given by $(x_1x_2 - y_1y_2) + i(x_1y_2 + x_2y_1)$. Hence cross correlation of 2 complex signals involves 4 multiply accumulates (MAC). However for auto-correlation this scales

down to 2 multiplications and 1 addition. Thus, we have

1 Complex MAC $=$ 4 Real MAC   for cross-correlations
1 Complex MAC $=$ 2 Real MAC   for auto-correlations

Hence, the total number of real N_{bit} multipliers required of for correlation of N_{sig} with N_{sig} is

$$
\begin{aligned}
N_X^r &= 4N_{sig}\left(\frac{N_{sig} - 1}{2}\right) + 2N_{sig} \\
&= 2N_{sig}^2 \qquad\qquad\qquad\qquad (17)
\end{aligned}
$$

Fourier Transform

The Discrete Fourier Transform (DFT) of a finite duration sequence $x(n)$ $0 \leq n \leq N - 1$ is given by

$$
X(k) = \sum_{n=0}^{N} x(n)W^{nk} \qquad (18)
$$

where $W = e^{-j(2\pi/N)}$, where W^{nk} is periodic in N. As seen from the equation for an N-point DFT the number of multiplications is N^2. Fast Fourier Transform or *FFT* is an alternative efficient algorithm to compute DFT. Using the straight forward pipelined Radix-2 implementation, the DFT equation can be broken down to $(N/2)(\log_2 N)$ butterfly stages of 4 multiples each. For a given input signal of bandwidth Δf, the *FFT* provides N_{bins} coefficients at the rate $\Delta f/N_{bins}$. Hence the total number of real $N_{bit} \times N_{bit}$ multiplications per second required is given as

$$
\begin{aligned}
N_X^{fft} &= 4(\Delta f/N_{bins})(N_{bins}/2)\log_2 N_{bins} \\
&= 2\Delta f \, \log_2 N_{bins} \qquad\qquad (19)
\end{aligned}
$$

Poly-phase Filter Bank

A Poly phase filter bank for a single node, single polarization consists of a FIR filter and a FFT module.

FIR Filter—The number of multiplications for a single FIR filter is equal to the number of taps (N_{taps}). For an input bandwidth Δf, the number of real multiplications required are $\Delta f N_{taps}$. For a complex signal the coefficients will also be complex, hence from (17) we have the total number of real multiplications for a complex signal as $4\Delta f N_{taps}$.

Filter Bank—Referring to (19), we have the total number of real multiplications required for a poly phase filter bank as

$$
\begin{aligned}
N_X^{pfb} &= 4\Delta f N_{taps} + 2\Delta f(\log_2 N_{bins}) \\
&= 2\Delta f(2N_{taps} + (\log_2 N_{bins})) \qquad (20)
\end{aligned}
$$

6. ACKNOWLEDGEMENTS
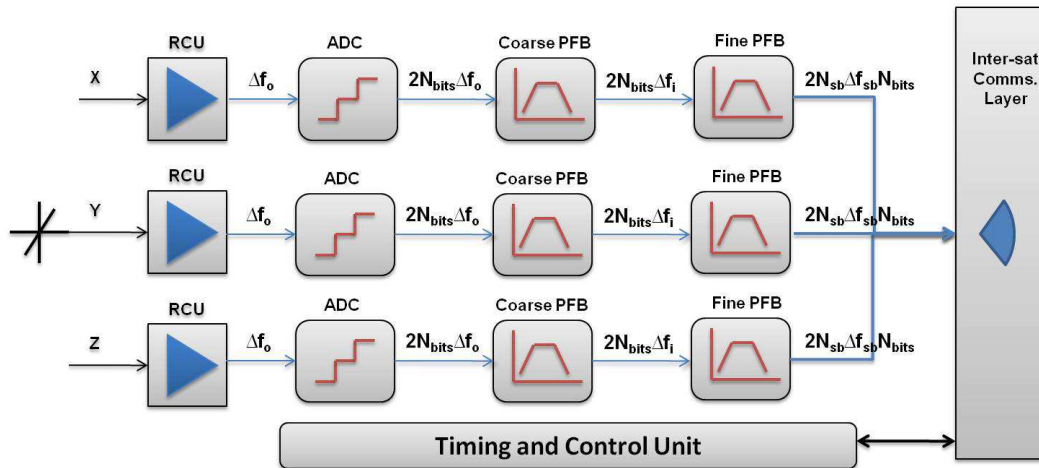
Figure 9. Node level Signal Processing (NSP) unit for OLFAR

REFERENCES

[1] S. Jester and H. Falcke, "Science with a lunar low-frequency array: From the dark ages of the Universe to nearby exoplanets," *nar*, vol. 53, pp. 1–26, May 2009.

[2] M. De Vos, A. Gunst, and R. Nijboer, "The lofar telescope: System architecture and signal processing," *Proceedings of the IEEE*, vol. 97, no. 8, pp. 1431–1437, aug. 2009.

[3] S. Ellingson, T. Clarke, A. Cohen, J. Craig, N. Kassim, Y. Pihlstrom, L. Rickard, and G. Taylor, "The long wavelength array," *Proceedings of the IEEE*, vol. 97, no. 8, pp. 1421–1430, aug. 2009.

[4] M. Bentum and A. Boonstra, "Low frequency astronomy - The challenge in a crowded RFI environment," in *General Assembly and Scientific Symposium, 2011 XXXth URSI*. IEEE, 2011, pp. 1–4.

[5] Weiler.K.W, Dennison.B.K, Johnston.K.J, Simon.R.S, Erickson.W.C, Kaiser.M.L, Cane.H.V, Desch.M.D, and Hammarstrom.L.M., "A low frequency radio array for space," *Astronomy and Astrophysics*, vol. 195, pp. 372–379, 1988.

[6] K. Weiler and D. Jones, "Low frequency astrophysics from space, summary of space initiatives to the radio/submm panel," Report, NRL USA, Report, February 1999.

[7] K. Weiler, *The promise of long wavelength radio astronomy*. AGU AMERICAN GEOPHYSICAL UNION, 2000, vol. 119.

[8] Jones, D.L. et al, "The astronomical low-frequency array (alfa)," in *IAU Colloquium 164L Radio Emission from Galactic and Extragalactic Compac Sources*, ser. ASP Conference Series, J. Zensus, G.B.Taylor, and J.M.Wrobel, Eds., vol. 144, 1998.

[9] R. T. Rajan, S. Engelen, M. Bentum, and C. Verhoeven, "Orbiting Low Frequency Array for Radio astronomy," in *IEEE Aerospace Conference*, March 2011, pp. 1–11.

[10] S. Engelen, C. Verhoeven, and M. Bentum, "OLFAR a radio telescope based on nano satellites in moon orbit," in *24th Annual Conference on Small Satellites, Utah, USA*. Utah State University, 2010.

[11] N. Saks, A.-J. Boonstra, R. T. Rajan, M. J. Bentum, F. Beilen, and K. van't Klooster, "DARIS, a fleet of passive formation flying small satellites for low frequency radio astronomy," in *The 4S Symposium (Small Satellites Systems & Services Symposium), Madeira, Portugal, 31 May - 4 June 2010 (ESA and CNES conference)*, 2010.

[12] R. T. Rajan, M. Bentum, and A. J. Boonstra, "Synchronization for space based ultra low frequency interferometry," in *IEEE Aerospace Conference, March 2-9, 2013, Big Sky, Montana US*, 2013.

[13] Romney.J.D, "Cross correlators," in *Synthesis Imaging in Radio Astronomy*, 1999.

[14] Y. Chikada, M. Ishiguro, H. Hirabayashi, M. Morimoto, K. Morita, T. Kanzawa, H. Iwashita, K. Nakazima, S. Ishikawa, T. Takahashi, K. Handa, T. Kasuga, S. Okumura, T. Miyazawa, T. Nakazuru, K. Miura, and S. Nagasawa, "A 6 x 320-MHz 1024-channel FFT cross-spectrum analyzer for radio astronomy," *Proc. IEEE*, vol. 75, no. 9, pp. 1203–1210, 1987.

[15] G. W. S. J. Richard Thompson.A, James M. Moran, *Interferometry and Synthesis in Radio astronomy*. KRIENGER, 1994.

[16] B. Gunst.A.W, Venema.L. B., "Distributed correlator for space applications," in *19th International Symposium on Space Terahertz Technology, Groningen*, 2008.

[17] Gunst.A.W, "Correlator configurations for interferometrs in space," in *New Perspectives for Post Herschel Infrared Astronomy for Space Workshop, Madrid, Spain*, 2008, presentation.

[18] L. R. B. Gold, *Theory and applications of digital signal processing*. Prentice-Hall Inc, 1975.

[19] L. R. D'Addario and C. Timoc, "Digital signal processing for the SKA: A strawman design," in *International SKA conference 2002, Groningen, The Netherlands*, August 2002. [Online]. Available: http://www.skatelescope.org/documents/memo25.pdf

BIOGRAPHY

Raj Thilak Rajan (S'10) received the B.Sc (with distinction) and M.Sc (with distinction) in Electronics science from University of Pune, India in 2004 and 2006 respectively. He is presently with the Digital and Embedded Signal Processing (DESP) R&D group at ASTRON, The Netherlands (since December 2008) and also a PhD candidate at Circuits And Systems (CAS), Faculty of EEMCS, TU-Delft, The Netherlands (since April 2010). Previously, he worked at Whirlpool (India), Politecnio di Bari (Italy) under MIUR and INFN fellowship, and was a visiting researcher at CERN (Switzerland) for the Compact Muon Solenoid (CMS) experiment in the Large Hadron Collider (LHC) project. His research interest lie in signal processing, algorithms and implementation.

Mark Bentum (S'92-M'95-SM'10) was born in Smilde, The Netherlands, in 1967. He received the M.Sc. degree in electical engineering (with honors) from the University of Twente, Enschede, The Netherlands, in August 1991. In December 1995 he received the Ph.D. degree for his thesis "Interactive Visualization of Volume Data" also from the University of Twente. From December 1995 to June 1996 he was a research assistant at the University of Twente in the field of signal processing for mobile telecommunications and medical data processing. In June 1996 he joined the Netherlands Foundation for Research in Astronomy (ASTRON). He was in various positions at ASTRON. In 2005 he was involved in the eSMA project in Hawaii to correlate the Dutch JCMT mm-telescope with the Submillimeter Array (SMA) of Harvard University. From 2005 to 2008 he was responsible for the construction of the first software radio telescope in the world, LOFAR (Low Frequency Array). In 2008 he became an Associate Professor in the Telecommunication Engineering Group at the University of Twente. He is now involved with research and education in mobile radio communications. His current research interests are short-range radio communications, novel receiver technologies (for instance in the field of radio astronomy), and sensor networks. Dr. Bentum is a Senior Member of the IEEE, the Dutch Electronics and Radio Society NERG, the Dutch Royal Institute of Engineers KIVI NIRIA, and the Dutch Pattern Recognition Society, Secretary of the Dutch URSI committee, Secretary of the Foundation of Scientific Activities of the Dutch URSI Committee, Executive Committee member of the IEEE Benelux Communications and Vehicular Technology Chapter, and has acted as a reviewer for various conferences and journals.

Andre Gunst was born in Havelte, The Netherlands, in 1972. He received the M.Sc degree in electrical engineering from the University of Twente, Enschede, The Netherlands, in June 1999. In the same year, he joined ASTRON as a digital system engineer with the R&D Department. Since 2004 he has worked extensively on the development of station systems for the LOw Frequency ARray (LOFAR) project and since 2006, he leads the LOFAR technical team. From 2010 onwards, he assumed a dual role, working for both ASTRON and the Square Kilometer Array (SKA) project. SKA will be the largest radio telescope on Earth, built in Australia or South-Africa. He is an Aperture Array Domain Specialist for the SKA office located in Manchester. In addition, he also leads the digital system development of several projects in ASTRON. His research interests include (digital) system design and digital signal processing.

Albert-Jan Boonstra was born in The Netherlands in 1961. He received the B.Sc. and M.Sc. degrees in applied physics from Groningen University, Groningen, the Netherlands, in 1984 and 1987, respectively. In 2005 he received the PhD degree for his thesis Radio frequency interference mitigation in radio astronomy from the Delft University of Technology, Delft, The Netherlands. He was with the Laboratory for Space Research, Groningen, from 1987 to 1991, where he was involved in developing the short wavelength spectrometer (SWS) for the infrared space observatory satellite (ISO). In 1992, he joined ASTRON, the Netherlands Foundation for Research in Astronomy, initially at the Radio Observatory Westerbork, Westerbork, The Netherlands. He is currently with the ASTRON R&D Department, Dwingeloo, The Netherlands, where he heads the DSP group. His research interests lie in the area of signal processing, specifically RFI mitigation by digital filtering.